Piping flow erosion in water retaining structures: inferring erosion rates from hole erosion tests and quantifying the failure time

Stéphane Bonelli, Nadia Benahmed

Piping flow erosion in water retaining structures: inferring erosion rates from hole erosion tests and quantifying the failure time

S. Bonelli and N. Benahmed

Cemagref, 3275 Route de Cezanne, CS 40061, 13182 Aix-en-Provence Cedex 5, France

E-mail: stephane.bonelli@cemagref.fr

Abstract

The piping flow erosion process, involving the enlargment of a continuous tunnel between upstream and downstream, is a major cause of water retaining structures. Such a pipe can be imputed to roots or burrows. The coefficient of erosion must be known in order to estimate the remaining time to failure and to downstream flood. The Hole Erosion test is a laboratory experiment especially suited to estimate a priori this geotechnical parameter. We propose therefore simplified expressions for the remaining time to breaching accounting for this erosion parameter. We established that the radius evolution of the pipe follows a two-parameters scaling law. The first parameter is the critical stress. The second parameter is the characteristic time of piping erosion, which is a function of the initial hydraulic gradient and the coefficient of erosion. We establish here new mechanically based relations for water retaining structures. The time to failure and the peak flow are related to the two basic parameters of piping failure: the coefficient of erosion, and the maximum pipe diameter prior to roof collapse and breaching. Orders of magnitude of the coefficient of erosion and the erosion rate are finally inferred from 18 case studies.

Introduction

The two most common failure modes of water retaining structures (earth-dams, dykes, levees) result from overtopping and piping. The breach due to failure generates a flood wave that propagates downstream the valley below the structure. Historically, the emphasis in dam safety has been on floods and overtopping. This case is fairly well documented [25]. However, the statistics of failure of embankment dams indicates that improvement in the understanding of piping is a significant concern of dam engineers. A comprehensive review of published literature on soil piping phenomena is presented by Richards and Reddy [17]. Piping accounts for 43% of all embankment dam failures, 54% for dams constructed after 1950 [10]. These statistics are based on the information reported in dam databases. Statistics concerning piping failures in dykes and levees are not yet avalaible.

The term “piping” is usually applied to a process that starts at the exit point of seepage and in which a continuous passage or pipe is developed in the soil by backward erosion, and enlarged by piping erosion. Evaluating the erodibility of a soil, both in terms of threshold of erosion (initiation) and rate of erosion (progression) are critical when evaluating the safety of a water retaining structure. Different soils erode at different rate. However, the relationship between the erosion parameters and the geotechnical and chemical properties of the soils remain unknown [7]. An overview of the research work on the erodibility of soils is presented in [23] and [24]. The three most common testing procedures used to evaluate the erodibility of soils are: 1) the Jet Erosion Test (JET) [13]-[14]; 2) the Erosion Function Apparatus (EFA) [4]; the Hole Erosion Test (HET) [23, 24].

The present study concerns the progression phase of the piping process: the enlargement of a tunnel. The hole erosion test appears to be an efficient and simple means of quantifying the erosion parameters. The experience acquired on more than 200 tests on several soils has confirmed what an excellent tool this test can be for quantifying the rate of piping erosion in a soil, and for finding the critical shear stress corresponding to initiation of piping erosion.

A model for interpreting the hole erosion test with a constant pressure drop was developed in [2] and [3]. A characteristic time of the internal erosion process was proposed, as a function of the initial hydraulic gradient, and the coefficient of erosion. It was shown that the product of the coefficient of erosion and the flow velocity is a significant adimensional number: when this number is small, the kinetic of erosion is low, and the concentration does not have any influence on the flow. This situation covers the main part of the available test results. Theoretical and experimental evidence was presented to the effect that the radius evolution of the pipe during erosion with constant pressure drop follows a scaling exponential law.

When piping erosion is suspected of occurring or has already been detected in situ, the rate of development is difficult to predict. In a growing number of cases, the location of population centers near the structure makes accurate prediction of breach parameters (namely the time to failure and the peak flow) crucial to the analysis. A critical analysis of the existing relationship was presented by Wahl [22]. These empirical relations are mostly straightforward regression relations that give the breach parameters as a function of various dam and reservoir parameters. It is questionable whether such relationships related to the reservoir storage, but not related to the rate of erosion, can be applied to estimate breach parameters for piping failure

scenarios. However, concerning piping failures, few investigators have attempted to relate the breach parameters to basic parameters. This paper aimed to establish new mechanically based relations relating the time to failure and the peak flow to the two basic parameters of piping failure: the coefficient of erosion, and the maximum pipe diameter prior to roof collapse. These relations make possible to infer orders of magnitude of the coefficient of erosion from field data.

Piping flow erosion

Piping flow erosion in cohesive soils

Piping occurs if $P_0 > \tau_c$ where P_0 is the driving pressure, equal to the tangential shear stress exerced by the piping flow on the soil, and τ_c is the critical stress.

The radius evolution of the pipe during erosion with constant pressure drop follows a scaling exponential law [3]:

$$R(t) = R_0\left[\frac{\tau_c}{P_0} + \left(1 - \frac{\tau_c}{P_0}\right)\exp\left(\frac{t}{t_{er}}\right)\right] \quad (1)$$

$$P_0 = \frac{R_0 \Delta p}{2L} \text{ (driving pressure)} \quad (2)$$

$$t_{er} = \frac{2\rho_{dry} L}{C_e \Delta p} \text{ (characteristing time of piping)} \quad (3)$$

where t_{er} is the characteristic time of piping erosion, R_0 is the initial radius, Δp is the pressure drop in the hole, L is the hole length, ρ_{dry} is the dry soil density, and C_e is the Fell coefficient of soil erosion.

The later is similar to the Temple and Hanson [20] coefficient of erosion k_d, as $k_d = C_e / \rho_{dry}$. The Fell erosion index is $I_e = -\log C_e$ (C_e given in s/m).

The Hole Erosion Test

The hole erosion test was designed to simulate piping flow erosion in a hole. This test is not new [15]. An eroding fluid is driven through the soil sample to initiate erosion of the soil along a pre-formed hole.

The results of the test are given in terms of the flow rate versus time curve with a constant pressure drop. Therefore, the flow rate is used as an indirect measurement of the erosion rate. For further details about this test, see [23]-[24].

The scaling law Equation (1) is compared with previously published data [23]-[24]. Analysis were performed in 18 tests, using 9 different soils (clay, sandy clay, clayey sand or silty sand). The initial radius and the length of the pipe were R_0 =3 mm and L =117 mm. Table 1 contains particle size distribution, and critical stress and Fell erosion index.

Figure 1 gives the effect of erosion process as the flow rate in relation to time, and shows that the use of t_{er} leads to efficient dimensionless scaling. Without this scaling, multiple graphs would be necessary to provide clarity of presentation. Scaled radius are plotted as a function of the scaling time in Figure 2. Nearly all the data can be seen to fall on a single curve. This graph confirms the validity of the scaling law Equation (1).

It is well known fact that different soils erode at different rate. Attemps were made to correlate erosion parameters - critical stress and coefficient of erosion - to common geotechnical or chemical soil properties in hope that simple equations could be developed for everyday use. All attemps failed to reach a reasonable correlation coefficient value [5].

It is strongly recommended carrying out hole erosion tests rather than using correlations, in order to evaluate the piping erosion parameters on any sample of cohesive soil from a site [23]-[24].

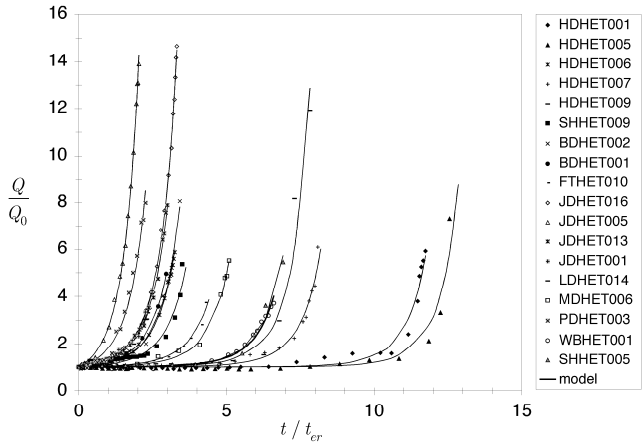

Figure 1: Hole Erosion Tests (symbols) versus scaling law (continuous lines). Dimensionless flow rate is shown as a function of dimensionless time.

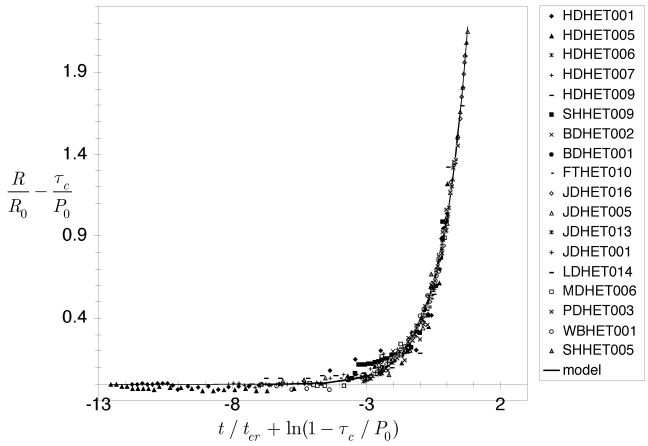

Figure 2: Hole Erosion Tests (symbols) versus scaling law (continuous lines). Dimensionless radius is shown as a function of dimensionless scaling time.

TABLE 1: HOLE EROSION TESTS, PROPERTIES OF SOILS SAMPLES, CRITICAL STRESS AND FELL EROSION INDEX

Soil		% Gravel	% Sand	% Fines	% <2μm	τ_c (Pa)	I_e
Lyell	silty sand	1	70	29	13	8	2
Fattorini	medium plasticity sandy clay	3	22	75	14	6	3
Pukaki	silty sand	10	48	42	13	13	3
Jindabyne	clayey sand	0	66	34	15	6 - 72	3 - 4
Bradys	high plasticity sandy clay	1	24	75	48	50 - 76	4
Shellharbour	high plasticity clay	1	11	88	77	99 - 106	4
Waranga	low plasticity clay	0	21	79	54	106	4
Matahina	low plasticity clay	7	43	50	25	128	4
Hume	low plasticity sandy clay	0	19	81	51	66 - 92	4 - 5

Mechanically based relations for the time to failure and the peak flow

The rate of erosion has a significant influence on the time for progression of piping and development of a breach in earth-dams, dykes or levees. This provides an indication of the amount of warning time available to evacuate the population at risk downstream of the dam, and hence has important implications for the management of dam safety.

Given that erosion has initiated, and the filters are absent or unable to stop erosion, the hydraulics of flow in concentrated leaks are such that erosion will progress to form a continuous tunnel (the pipe). We consider the case of a straight and circular pipe, of current radius $R(t)$, in an embankment of heigth H_{dam} and base width $L_{dam} = c_L H_{dam}$ (Figure 3). The average quantities are defined as follows:

$$L(t) = c_L\left[H_{dam} - R(t)\right] \text{ (current pipe length)} \quad (4)$$

$$\Delta p_T(t) = \rho_w g\left[\Delta H_w - R(t)\right] \text{ (average pressure drop)} \quad (5)$$

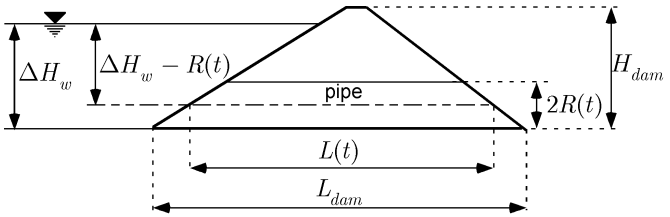

Figure 3: Sketch of the piping erosion in a water retaining structure.

Although the head drop is likely to decrease with time, the situation for the case $\Delta H_w = H_{dam}$ is more critical and, therefore, yields a conservative estimate of the time needed to initiate roof collapse. The rate of pipe enlargement is highly dependent on the erodibility of the soil as measured by the coefficient of erosion C_e. The enlargement of the pipe causes roof collapse and creates a breach. The scaling law of the piping erosion process with a constant hydraulic gradient is given in Equation (1). We can now propose an expression for the remaining time to breaching. The piping process begins at time t_0 with the initial radius R_0, both unknown.

A sketch of our description is represented in Figure 4. A visual inspection defines the initial time $t_d > t_0$ for detection, and can provide an estimation of the output flow rate, thus an estimation of the radius $R_d > R_0$. We take R_u and t_u to denote the maximum radius of the pipe before roof collapse, and the collapse time, respectively. For $t > t_u$, the piping failure continues to cause erosion in a similar way to an overtopping failure. The modeling of the overtopping breaching is fairly well documented [25].

The erosion onset radius can be neglected, as $R_d \ll R_u$. The remaining time prior to breach $\Delta t_u = t_u - t_d$ can therefore be estimated as follows

$$\Delta t_u \approx t_{er} \ln\left(\frac{R_u}{R_d}\right) \quad (6)$$

This important result establishes that the coefficient of erosion C_e can serve as an indicator of the remaining time to breaching, as $\Delta t_u \propto C_e^{-1}$. The peak flow is assumed to correspond to the maximum radius of the pipe. Consequently, the time prior to breach Δt_u is also the time from detection (e.g. eyewitnesses observations) to peak discharge.

The average quantities are defined as follows:

$$\Delta p_T(t) = \frac{1}{2} k \rho_w V^2(t) + \Delta p(t) \quad (7)$$

$$\tau_b(t) = \frac{R(t)\Delta p(t)}{2L(t)} \text{ (tangential stress)} \quad (8)$$

$$V(t) = \sqrt{\frac{\tau_b(t)}{f_b \rho_w}} \text{ (velocity)} \quad (9)$$

$$Q(t) = \pi R(t)^2 V(t) \text{ (peak flow)} \quad (10)$$

where k is the singular head loss coefficient (section sharpening of the pipe inlet), and f_b is the turbulent friction factor in the pipe.

Inserting Equations (4)-(9) in Equation (10) yields:

$$Q_{peak} = \pi R_u^{5/2} \sqrt{\frac{2g(\Delta H_w - R_u)}{kR_u + 4 f_b c_L (H_{dam} - R_u)}} \qquad (11)$$

It is emphasized that Equations (6) and (11) do not relate Δt_u and Q_{peak} to the reservoir storage, which is mechanically irrelevant, as it is usually proposed in the dam engineering litterature. In other hand, Δt_u and Q_{peak} are directly related to R_u. The relations Equations (6) and (11) are therefore not useful as predictors if R_u cannot be estimated with great certainty prior to a breach.

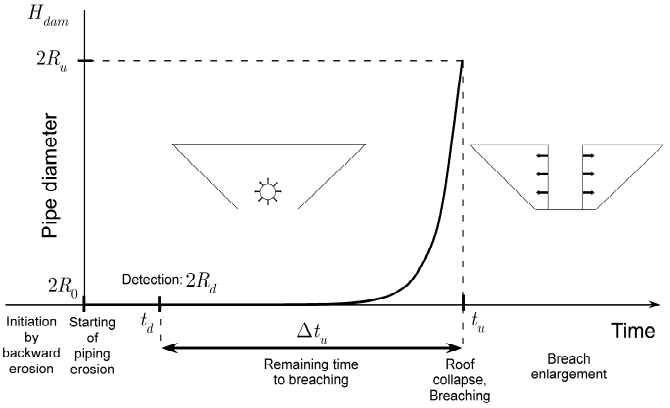

Figure 4: Piping erosion in a water retaining structure, phases from initiation to breaching.

Order of magnitude of mechanical quantities on case studies

Case study data provide only limited information. This is primarly due to the variations in interpretation of failure by the lay person who often is the only eyewitness to a dam failure. In the best case, the only information available are the time to breaching and the peak flow. The radius or the flow rate at detection is never reported. Inverting Equation (6) yields

$$C_e \approx \frac{2\rho_{dry} L}{\Delta t_u \Delta p} \ln\left(\frac{R_u}{R_d}\right) \qquad (12)$$

Few attemps have been made to propose a constitutive model to calculate the radius value prior to roof collapse. This estimate can be made on the basis of information derived from the peak flow value Equation (11). If the peak flow is unknown, an upper bounds can however be obtained by taking $R_u = H_{dam}/2$:

$$C_e < \frac{2\rho_{dry} L}{\Delta t_u \Delta p} \ln\left(\frac{H_{dam}}{2R_d}\right) \qquad (13)$$

The present statement is not intended to provide accurate values of the shear stress, the velocity or the flow rate. Rather, attention is focused explicitely on the more limited goal of giving numbers, and orders of magnitude.

Tables 1 and 2 contain data and results of this simplified analysis on 14 well documented piping failures cases. These cases were taken from the database presented in [22], where data on 108 case studies of actual embankment dam failures were collected from numerous sources in the literature.

The dam height H_{dam} ranged from 6 m to 93 m. The relative water level $\Delta H_w / H_{dam}$ at failure ranged from 0.48 to 1. The coefficient $c_L = L_{dam} / H_{dam}$ ranged from 1.54 to 3. The failure time Δt_u ranged from 0.5 h to 5.25 h. The peak flow Q_{peak} ranged from 79 m^3/s to 65,120 m^3/s. The relative maximum radius $2R_u / H_{dam}$ estimated with Equation (11) ranged from 0.26 to 0.96.

The shear stress τ_b Equation (6) at failure (prior to roof collapse) ranged from 262 Pa to 8,051 Pa. The water velocity at failure V Equation (7), estimated with $k = 0.5$ and f_b =0.005, ranged from 7 m/s to 40 m/s.

The choice of k, the singular head loss coefficient, corresponds to the section sharpening of the pipe inlet. The choice of f_b is consistent with the Reynold number at failure, which ranged from 3×10^7 to 2×10^9. This estimate was obtained on the basis of investigations with several friction factor formula [1, 16, 19].

The radius at detection R_d is unknown. As $R_d \ll \Delta H_w \leq H_{dam}$, the flow rate can roughly be estimated with $Q(R_d) \approx \pi R_d^{5/2} \sqrt{g/(2 f_b c_L)}$. This gives $Q \approx 1$ m^3/mn for R_d =4 cm and $Q \approx 1$ m^3/s for R_d =20 cm. These values can be considered as two extreme values for visual detection and emergency status.

The erosion index rate $I_e = -\log C_e$ was estimated as an average of four numbers, calculated with the RHS of Equations (12) and (13), with R_d =20 cm and R_d =4 cm. The average erosion index rate was found to range from 1.6 to 3.0. The standard deviation ranged from 0.08 to 0.22.

Wan and Fell [23, 24] found that the coefficient of erosion C_e can differ by up to 10^5 times across different soils from a serie of hole erosion tests (13 soils). The coefficient of erosion was found to range from 10^{-6} $s.m^{-1}$ to 10^{-1} $s.m^{-1}$.

In this study dealing with piping erosion, the coefficient of erosion C_e inferred from data of case histories ranged from 10^{-3} $s.m^{-1}$ to 10^{-2} $s.m^{-1}$. Our results are consistent with previous finding.

For overtopping, Courivaud and Fry [6] reported values of breach widening rate inferred from data of 10 case histories, covering a range of dam height from 8 m to 60 m. These values ranged from 14 $cm.min^{-1}$ to 600 $cm.mn^{-1}$. For piping flow erosion, the erosion rate prior to roof collapse can be estimated with $V_{er} = \tau_b C_e / \rho_{dry}$ and ρ_{dry} =1,600 kg/m^3. We found that V_{er} ranged from 3 $cm.min^{-1}$ to 107 $cm.min^{-1}$. These comparisons confirm the validity of our statement: orders of magnitude can be inferred from field data with limited information.

Conclusion

Few attempts have been made so far to model the piping erosion process in soils. A simplified but mechanically based approach was used to establish new relationship for water retaining structures. The time to piping failure and the peak flow were related to the coefficient of erosion, and the maximum pipe diameter prior to roof collapse and breaching. Several mechanical quantities were inferred from 14 case studies: the shear stress, the velocity, the coefficient of erosion and the erosion rate. This is the first attempt to derive such numbers from field data for the piping erosion process. The comparisons with published data on erosion confirmed that the obtained orders of magnitude, inferred from case studies with limited information, are relevant.

For water retaining structures, the coefficient of erosion is the first important parameter: it can serve as an indicator of the remaining time to breaching, but visual detection of the piping event and reporting is required. This coefficient can be obtained with the Hole Erosion Test. However, the issue of the way the change of scale (from the laboratory to the structure) could affect the coefficient of erosion remains to be adressed.

The second important parameter is the maximum pipe diameter prior to roof collapse and to breaching. It can serve as an indicator of the peak flow. However, constitutive relations to calculate this diameter as a function of mechanical quantities (such as the soil shear strength) are currently limited. To date, this information cannot be estimated with great certainty prior to a breach.

Acknowledgements

This project was sponsored by the National French Research Programme ERINOH.

References

[1] Barenblatt G.I., Chorin A.J., Prostokishin V.M. (1997). *Scaling laws for fully developed turbulent flow in pipes*. Applied Mechanics Reviews. Vol. 50, No. 7, pp. 413-429.

[2] Bonelli S., Brivois O., Borghi R., Benahmed N. (2006). *On the modelling of piping erosion*. Comptes Rendus de Mécanique. Vol. 8-9, No. 334, pp. 555-559.

[3] Bonelli S., Brivois O. (2008). *The scaling law in the hole erosion test with a constant pressure drop*. International Journal for Numerical and Analytical Methods in Geomechanics. Vol. 32, pp. 1573-1595.

[4] Briaud J.L, Ting F.C.K., Chen H.C., Cao Y., Han S.W., Kwak K.W. (2001). *Erosion Function Apparatus for Scour Rate Predictions*. Journal of Geotechnical and Geoenvironmental Engineering. Vol. 127, No. 2, pp. 105-113.

[5] Briaud J.-L. (2006). *Chapter 9 - Erosion tests on New Orleans levee samples*, in *Investigation of the performance of the New Orleans protection systems in Hurricane Katrina on August 29, 2005*. Final report July 31.

[6] Courivaud J.-R., Fry J.-J. (2007). *Dam breaching, Case studies*, in *Assessment of the Risk of Internal Erosion of Water Retaining Structures: Dams, Dykes and Levees*, Report of the European Working Group of ICOLD, Technische Universitat Munchen (TUM), No 114, Munich, pp. 245-254.

[7] Fell R, Fry J-J. (2007). *Internal Erosion of Dams and Their Foundations*. Taylor & Francis, London.

[8] Froehlich D.C. (1995). *Embankment dam breach parameters revisited*. Proceedings of the 1995 ASCE Conference on Water Resources Engineering, San Antonio, Texas, August, pp. 887-891.

[9] Froehlich D.C. (1995). *Peak Outflow from Breached Embankment Dam*. Journal of Water Resources Planning and Management. Vol. 121, No. 1, pp. 90-97.

[10] Foster M., Fell R., Spannagle M. (2000). A *method for assessing the relative likelihood of failure of embankment dams by piping*. Canadian Geotechnical Journal. Vol. 37, pp. 1025–1061.

[11] Foster M., Fell R., Spannagle M. (2000). *The statistics of embankment dam failures and accidents*. Canadian Geotechnical Journal. Vol. 37, pp. 1000–1024.

[12] Hanson G. J. (1991). *Development of a jet index to characterize erosion resistance of soils in earthen spillways*. Transactions of the ASAE. Vol. 34, No. 5, pp. 2015-2020.

[13] Hanson G. J., Cook. K.R. (2004). *Apparatus, Test Procedures, and Analytical Methods to Measure Soil Erodibility In Situ*. ASAE Applied Engineering in Agriculture. Vol. 20, No. 4, pp. 455-462.

[14] Hanson G.J., Simon A. (2001). *Erodibility of cohesive streambeds in the loess area of the midwestern USA*. Hydrological Processes. Vol. 15, No. 1, pp. 23-38

[15] Lefebvre G., Rohan K., Douville S. (1985). *Erosivity of natural intact structured clay : evaluation*. Canadian Geotechnical Journal. Vol. 22, pp. 508-517.

[16] Mc Keon B.J., Zagarola M.V., Smits A.J. (2005). *A new friction factor relationship for fully developed pipe flow*. Journal of Fluid Mechanics. Vol. 538, pp. 429-443.

[17] Richards K.S., Reddy K.R. (2007). *Critical appraisal of piping phenomena in earth dams*. Bulletin of Engineering Geology and the Environment. Vol. 66, No 4, pp. 381-402.

[18] Rohan K., Lefebvre G., Douville S., Milette J.-P. (1986). *A new technique to evaluate erosivity of cohesive material*. Geotechnical Testing Journal. Vol. 9, No 2, pp. 87-92.

[19] Shockling M.A., Allen J.J., Smits A.J. (2006). *Roughness effects in turbulent pipe flows*. Journal of Fluid Mechanics. Vol. 564:267-285.

[20] Temple D.M., Hanson G.J. (1994). *Headcut development in vegetated earth spillways*. Applied Engineering in Agriculture. Vol. 10, No 5, pp. 677-682.

[21] Wahl T.L. (2004). *Uncertainty of predictions of embankment dam breach parameters*. Journal of Hydraulic Engineering ASCE. Vol. 130, No 5, pp. 389-397.

[22] Wahl T.L. (1998). *Prediction of embankment dam breach parameters—a literature review and needs assessment*. Dam Safety Rep No. DSO-98-004, US Dept. of the Interior, Bur of Reclamation, Denver, CO.

[23] Wan C.F, Fell R. (2004). *Investigation of rate of erosion of soils in embankment dams*. Journal of Geotechnical and Geoenvironmental Engineering. Vol. 130, No 4, pp. 373-380.

[24] Wan C.F, Fell R. (2004). *Laboratory Tests on the Rate of Piping Erosion of Soils in Embankment Dams*. Geotechnical Testing Journal. Vol. 27, No 3, pp. 295-303.

[25] Wang Z., Bowles D.S. (2007). *A numerical method for simulating one-dimensional headcut migration and overtopping breaching in cohesive and zoned embankments*. Water Resources Research. Vol. 3, W05411.

TABLE 2: WELL DOCUMENTED PIPING FAILURE CASES. THE FIRST FIVE COLUMNS ARE TAKEN FROM [23]. THE MAXIMUM RADIUS IS ESTIMATED BY USING EQ. (11)

Dam name and location	H_{dam} (m)	ΔH_w (m)	c_L	Δt_u (h)	Q_{peak} ($m^3.s^{-1}$)	R_u (m)
Ireland No. 5, Colo.	6.0	3.8	3.0	0.5	110	2.20
Lower Latham, Colo.	8.6	5.8	3.0	1.5	340	3.53
Frankfurt, Germany	9.8	8.2	3.0	2.5	79	1.42
Kelly Barnes, Ga.	11.6	11.3	1.7	0.5	680	3.66
French Landing, Mich.	12.2	8.5	2.8	1.16	929	5.30
Lake Latonka, Penn.	13.0	6.3	2.2	3	290	3.05
Lake Avalon, N.M.	14.5	13.7	2.9	2	2,320	6.94
Quail Creek, Utah	18.9	16.7	3.0	1	3,110	7.53
Hatchtown, Utah	19.2	16.8	2.3	4	3,080	7.40
Little Deer Creek, Utah	26.2	22.9	2.4	0.66	1,330	4.37
Bradfield, England	29.0	29.0	1.7	0.5	1,150	3.75
Apishapa, Colo.	34.1	28.0	2.4	3.25	6,850	9.51
Hell Hole, Calif.	67.1	35.1	1.5	0.75	7,360	9.30
Teton, Idaho	93.0	77.4	2.7	5.25	65,120	22.73

TABLE 3: WELL DOCUMENTED PIPING FAILURE CASES. COEFFICIENT OF EROSION AND FINAL EROSION RATE ESTIMATES. THE EROSION INDEX RATE IS $I_{er} = -\log C_e$

Dam name and location	τ_b (Pa)	V_u ($m.s^{-1}$)	I_{er} (mean	±std. dev.)	C_e (10^{-3} $s.m^{-1}$)	V_{er} ($cm.mn^{-1}$)
Ireland No. 5, Colo.	262	7	1.6	±0.13	24	24
Lower Latham, Colo.	379	9	2.0	±0.11	10	14
Frankfurt, Germany	784	13	3.0	±0.22	1	3
Kelly Barnes, Ga.	1,309	16	2.0	±0.12	10	47
French Landing, Mich.	552	11	1.8	±0.09	15	31
Lake Latonka, Penn.	490	10	2.5	±0.14	4	6
Lake Avalon, N.M.	1,175	15	2.2	±0.08	6	25
Quail Creek, Utah	1,524	17	2.0	±0.09	10	56
Hatchtown, Utah	1,606	18	2.6	±0.09	2	14
Little Deer Creek, Utah	2,454	22	2.3	±0.15	5	48
Bradfield, England	3,378	26	2.4	±0.16	4	54
Apishapa, Colo.	2,902	24	2.7	±0.10	2	24
Hell Hole, Calif.	3,662	27	2.1	±0.13	8	107
Teton, Idaho	8,051	40	2.9	±0.09	1	42